Heliyon 10 (2024) e32608

Contents lists available at ScienceDirect

Heliyon

journal homepage: www.cell.com/heliyon

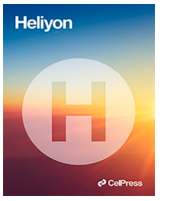

Research article

Experimental study of the two-phase flow distribution in helical-structured vertical headers

Moojoong Kim [a,*], Jongsoo Jeong [b], Kiyoshi Saito [b], Sangmu Lee [c], Hyunyoung Kim [c]

[a] Research Institute for Science and Engineering, Waseda University, Shinjuku-ku, Tokyo, 169-8555, Japan
[b] Department of Applied Mechanics and Aerospace Engineering, Waseda University 3-4-1 Okubo, Shinjuku-ku, Tokyo, 169-8555, Japan
[c] Samsung Research and Development Institute Japan, Osaka 562-0036, Japan

ARTICLE INFO

Keywords:
Microchannel heat exchanger
Flow distribution
Helical header structure
Vertical header
Maldistribution

ABSTRACT

A vertical header is a crucial component of a microchannel heat exchanger that facilitates the distribution of the two phases of the refrigerant into horizontally aligned channels. Ensuring an even distribution of the refrigerant into the channels is imperative for achieving the designed optimal performance. Previous studies have indicated that the distribution characteristics of the vertical header are contingent upon the mass flow rate and geometric properties of the header. This study aims to investigate the distribution characteristics of two-phase flow resulting from structural modifications in the header, specifically by implementing a vertical header with a helical structure. Hence, an experimental device simulating a microchannel heat exchanger found in a commercial air conditioning system was employed. The distribution characteristics of the vertically oriented header with a helical structure were measured by varying the inlet conditions (mass flow rate: 50–100 kg h^{-1}; vapor quality: 0.1–0.2). The measured distribution characteristics were compared with those obtained from a conventional straight vertical header possessing the same cross-sectional properties. The experimental findings demonstrated that the helical structure induced a distinctive flow pattern and facilitated the mixing of the two phases. Furthermore, this helical structure exhibited reduced inertial forces compared to the simple vertical header, leading to improved distribution performance.

1. Introduction

Microchannel heat exchangers (MCHX) have attracted significant interest recently due to their high surface density and compact design [1,2]. These heat exchangers offer several advantages over traditional finned tube heat exchangers. Their small size enables them to achieve the desired performance while minimizing the charge requirements of the refrigerant [3]. Hence, MCHX are widely used in heating, ventilating, and air-conditioning (HVAC) and cooling applications, ranging from small-scale to large-scale systems [4–6]. Unlike finned tube heat exchangers, microchannel heat exchangers are characterized by a vertical header and parallel channels stemming from the vertical header.

Typically, MCHXs with vertical headers are used in outdoor airconditioning units, where they serve as evaporators in heat-pump cycles. In the evaporator operation mode, a two-phase refrigerant with a vapor quality ranging from 0.1 to 0.2 is introduced into the vertical header and distributed into parallel channels. The two-phase flow within MCHX is characterized by gas and liquid phases,

* Corresponding author.
E-mail address: mj_kim@aoni.waseda.jp (M. Kim).

https://doi.org/10.1016/j.heliyon.2024.e32608
Received 25 February 2024; Received in revised form 5 June 2024; Accepted 6 June 2024
Available online 17 June 2024

Nomenclature

A	header cross-cut area (m^2)
C	correlation coefficient
D_h	hydraulic diameter of header (m)
De	Dean number
Fr	Froude number
G	mass flux (kg m^{-2} s^{-1})
g	gravity (m s^{-2})
i	specific enthalpy (kJ kg^{-1})
i_f	specific enthalpy of saturated liquid (kJ kg^{-1})
i_{fg}	specific enthalpy of vaporization (kJ kg^{-1})
L	characteristic length (m)
$\dot{m}$	mass flow rate (kg s^{-1})
P	pressure (kPa)
p	helical structure pitch (m)
Q	power consumption (kW)
R_c	curvurture radius (m)
Re	Reynolds number
r	helical radius (m)
T	temperature ($^{\circ}$C)
x	vapor quality *Greek symbols*
ρ	density (kg m^{-3})
μ	dynamic viscosity (Pa s) *Subscripts*
g	gas
h	header
i	tube index $(1, 2, \ldots 5)$
in	inlet
j	phase index (l, v)
l	liquid phase
n	number of tube
ph	preheater
s	superheated gas heater
sat	saturation
tp	two-phase mixture
ts	test section
v	vapor phase

exhibiting variations in density, velocity, and buoyancy. Consequently, this leads to a separated flow pattern within the vertical header, resulting in a non-uniform distribution of refrigerant. Refrigerant flow maldistribution between the bifurcated channels can give rise to localized dry-out, system degradation, and, ultimately, heat exchanger failure [7]. Therefore, employing different strategies to address and mitigate long-term flow maldistribution issues is imperative.

In a single-phase flow, the flow distribution within the header is primarily governed by the pressure drop resulting from friction within the tubes [8–10]. However, in the case of two-phase flow, the flow distribution can be influenced by several factors due to the inherent complexity of such flow regimes. A combination of experimental and theoretical approaches has been employed to gain a comprehensive understanding of two-phase flow distribution. These approaches characterize various aspects, including the structural and geometric design, operating conditions (mass flow rate, inlet quality, flow pattern, and heat load), and working fluid [11–13].

Siddiqui and Zubair [14] emphasized the significance of considering the structural parameters of the vertical header to achieve a uniform flow distribution. Lee [15] studied a compact heat exchanger featuring vertical headers and confirmed that the recirculation of the two-phase flow toward the upper section of the vertical header plays a crucial role in influencing flow distribution. Hwang et al. [16] and Redo et al. [17,18] conducted studies indicating that two-phase inlet conditions (mass flow rate and vapor quality) at the header inlet have a significant impact on flow distribution. Higher mass flow rates and lower vapor qualities effectively produced uniform flow distribution. Regarding the combination of structural design and operating conditions, Kim et al. [19] demonstrated that a reasonable flow distribution can be achieved by considering the physical configuration of the vertical header (cross-sectional area, height, and outlet bore) and operating conditions (mass flow rate, vapor quality, and temperature). Furthermore, Fei and Hrnjak [20] highlighted the importance of flow patterns, influenced by the mass flux and working fluid properties, particularly in horizontal headers under the influence of gravity.

While previous studies have predominantly focused on conventional vertical or horizontal headers with typical structures, only a few studies have explored novel structures to improve flow distribution. Recognizing that the uneven distribution in the header arises

from the separated characteristics of the two-phase flow, it may be meaningful to explore active structural improvements that can suppress the separated flow (e.g., mixed flow) and promote mixed flow. Mansour et al. [21] numerically examined the mixing effects of two hypothetical fluids flowing through a helical coil. The flow inside the helical coil exhibits a distinctive counter-rotating flow (Dean vortex) in the direction of the flow cross-section, which enhances mixing between two fluids or two phases. Karali et al. [22] investigated the effect of tapered longitudinal section manifolds on flow distribution uniformity. The flow distribution for different manifold taper ratios (the diameter ratio of both ends of the manifold) was derived numerically. Although the study is for a single-phase, there exists an optimal manifold ratio depending on the inlet flow rate for a novel structured header, which is related to the pressure drop.

As discussed in the previous literature, a header with a novel structure can be a key parameter to improve flow distribution. Nevertheless, experimental studies have been scarce due to the fabrication of headers with special structures and the experimental difficulty of achieving two-phase flow. In this study, we experimentally analyzed the flow distribution characteristics of a vertical header with a helical structure that can be applied to MCHX with two-phase flow. In this study, experimental measurements were conducted under three mass flow conditions (50, 100, and 150 kg h^{-1}) and two inlet vapor quality conditions (0.1 and 0.2). The flow distribution characteristics obtained from the helical-structured vertical header were compared to those obtained from a previous study [19] using a header with the same height and cross-sectional geometry but lacking the helical structure. Additionally, dimensionless numbers were analyzed to gain insights into the behavior of the two-phase flow through the helical structure.

2. Experimental investigation

2.1. Helical-structured vertical header

Fig. 1 shows the helical-structured vertical header. The parallel tube connected to the header outlet was simplified to a smooth tube with a pressure control valve to directly compare with the findings with those of our previous work [19]. Fig. 1(a) illustrates the fabricated vertical header, which incorporated five 57.5 × 58.5 mm sight glasses strategically positioned along the flow direction within the header. These sight glasses allow us to observed the internal flow dynamics. A metal rod (φ15.88 mm) with a pitch (p) of 105 mm was machined to create the helical-structured channel, defining the flow path inside the header, as shown in Fig. 1(b). Through the sight glass, the helical channel inside can be observed as shown in Fig. 1(c), and the two-phase fluid follows the helical channel to the top (see red arrow). The cross-sectional geometry of the helical-structured channel (see Fig. 1(d)) is identical to that of the simple straight vertical header employed in our previous study [19]. The inlet and outlet of the vertical header were oriented in the

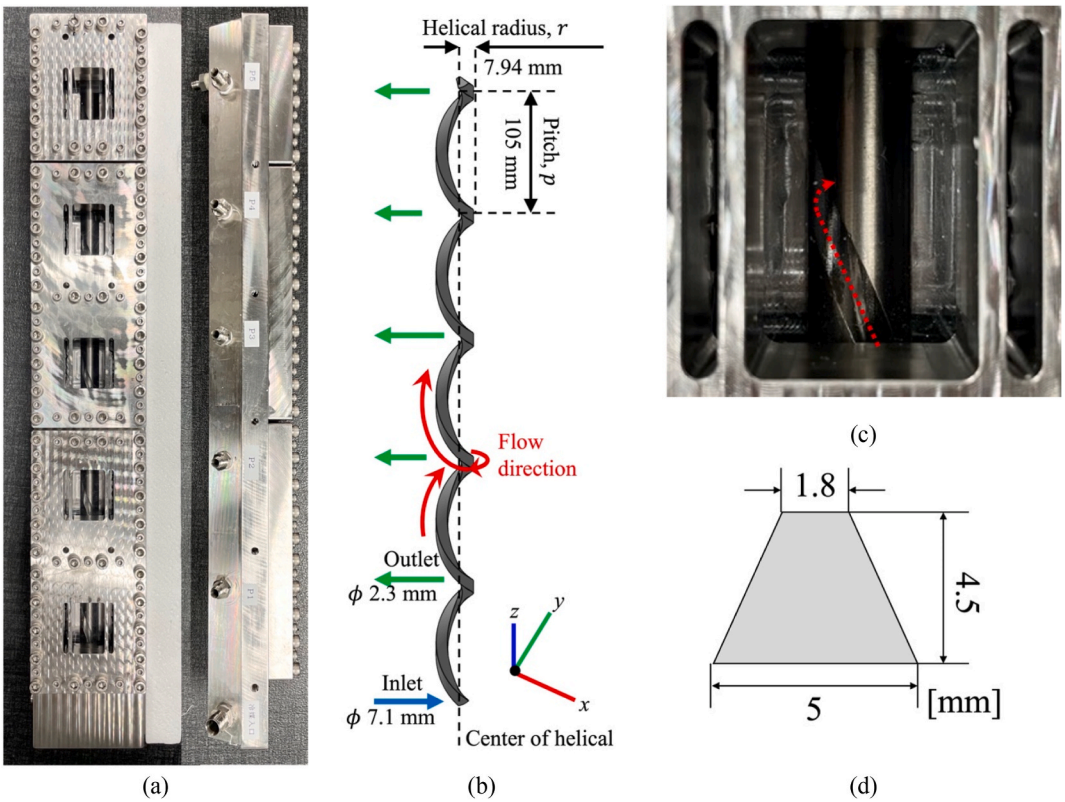

Fig. 1. Helical-structured vertical header: (a) fabricated vertical header, (b) inside the helical structure, and (c) cross-section of the helical-structured channel.

same direction. Copper tubes with inner diameters of 7.1 mm and 2.3 mm were used for the inlet and outlet, respectively. The spacing between the five outlets was designed to be 105 mm, matching the pitch of the helical-structured channel. Furthermore, the distance between the first and fifth outlets was 420 mm, consistent with the configuration employed in our previous work [19]. Considering the pitch of the channel, the distance between the first outlet and the header inlet was 105 mm.

2.2. Experimental apparatus and conditions

Fig. 2 depicts the configuration of the experimental setup, including the vertical header. Detailed specifications of the experimental apparatus, including the individual instruments, can be found in our previous work [19], and are therefore only briefly presented here. The refrigerant loop, except for the test section, consists of copper tubing with an inner diameter of 7.1 mm. After passing through the subcooler, the refrigerant is transported from the receiver tank to the test section using a magnetic geared pump (MML series, SANWA), where it is adjusted to a two-phase condition with a specific inlet vapor quality via a preheater. After leaving the test section, the refrigerant is condensed in the after condenser and returned to the receiver tank. The newly designed helical-structured vertical header is installed as the front header, and tubes 1–5 are connected to the header outlet. Three valves installed in each branch tube are used to measure the flow rate and quality of the vapor flowing through the individual branch tubes. The entire refrigerant loop is insulated (Aeroflex®) with a thickness of 10 mm to reduce heat loss to the surrounding environment. The sensor instruments used for the measurements are summarized in Table 1. The uncertainty associated with the generation of the inlet vapor quality condition for the experimental apparatus was ±5.17 % ($x = 0.2$, 15 °C, 100 kg h^{-1}).

Three mass flow rates (50, 100, and 150 kg h^{-1}; corresponding mass fluxes: 908, 1815, and 2723 kg m^{-2} s^{-1}) and two inlet vapor quality (0.1 and 0.2) conditions were selected for the experimental apparatus and vertical header. The experimental conditions were identical to those in our previous study [19], which aimed to simulate the operating conditions of an evaporator in a residential heat-pump system. The working fluid used in the experiments was R410A, with a saturation temperature and pressure of 15 °C and 1.2584 MPa, respectively. Table 2 summarizes the experimental conditions.

2.3. Measurement procedure and data reduction

The measurement procedure used in this experiment was established in our previous study [19]. The mass flow rate ($\dot{m}_i$) and vapor quality (x_i) of each branch tube were measured along the bypass line. Once a steady state was achieved for each experimental condition, the pressure drop (ΔP_i) in each tube was measured and used as the reference pressure drop for determining the mass flow rate of each tube. The gas heater was employed to convert the two-phase flow of a specific tube through the bypass into a superheated

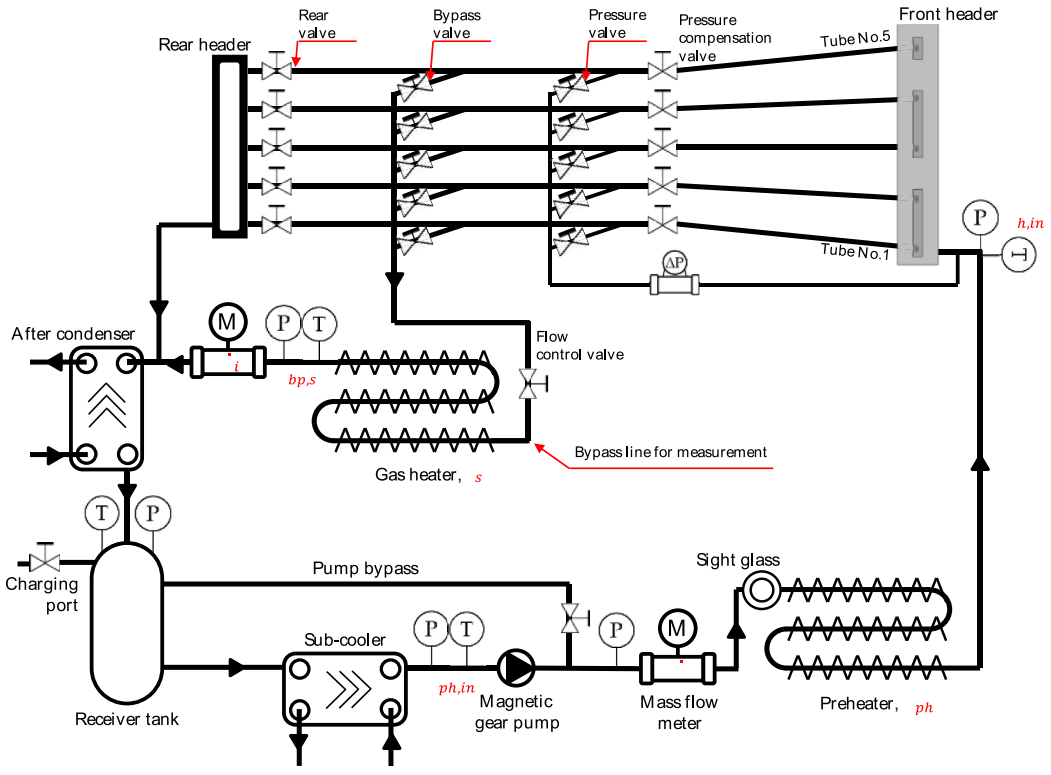

Fig. 2. Schematic diagram of the experimental setup [19].

Table 1
Summary of the experimental sensor instruments.

Instrument	Variable	Model	Accuracy
Liquid Coriolis flowmeter	Entire flow rate	OVAL, ALTImass II type U	±0.05 % of rdg.
Vapor Coriolis flowmeter	Individual flow rate	OVAL, ALTImass II type U	±0.05 % of rdg.
Power analyzer	Power consumption	HIOKI, PW3336	±0.15 % of rdg.
Pressure transmitter	Pressure	YOKOGAWA, FP101A	±0.25 % of F·S.
Differential pressure transmitter	Differental pressure	Azbil, JTD920A	±0.1 % of F·S.
PT100 RTD	Temperature	SAKAGUCHI, Class A	±0.15 °C

Table 2
Summary of experimental inlet conditions.

Variable	Conditions
Mass flow rate, $\dot{m}$ (kg h^{-1})	50, 100, 150
Inlet vapor quality, $x_{h,in}$	0.1, 0.2
Saturation temperature, T_{sat} (°C)	15
Saturation pressure, P_{sat} (MPa)	1.2854
Refrigerant	R410A

single-phase gas. The power consumption (Q_s) of the gas heater, temperature (T_s), and pressure (P_s) at the end of the bypass were recorded for vapor quality measurements. The pressure drop in each tube was maintained at the reference pressure drop while measuring the mass flow rate and vapor quality through the bypass. The abovementioned procedure was repeated for all branch tubes, and the individual vapor quality measurements were associated with an uncertainty of ±8.42 %.

Based on the data collected using the procedure mentioned above, the inlet vapor quality ($x_{h,in}$) and individual vapor quality (x_i) were derived as follows:

The inlet vapor quality ($x_{h,in}$) was calculated using Equation (1).

$$x_{h,in} = \frac{i_{h,in} - i_f\big|_{T_{h,in}}}{i_{fg}\big|_{T_{h,in}}} \tag{1}$$

where $i_{h,in}$, $i_f\big|_{T_{h,in}}$, and $i_{fg}\big|_{T_{h,in}}$ correspond to the specific enthalpy, saturated-liquid-specific enthalpy, and specific latent enthalpy of the two-phase inlet state, respectively. Furthermore, $i_{h,in}$ can be derived from the specific enthalpy of the subcooled refrigerant at the front of the preheater ($i_{ph,in}$), mass flow rate into the header ($\dot{m}$), and power consumption of the preheater (Q_{ph}), as shown in Equation (2).

$$i_{h,in} = i_{ph,in} + \frac{Q_{ph}}{\dot{m}} \tag{2}$$

x_i can be derived as shown in Equation (3).

$$x_i = \frac{\dot{m}_i\left(i_{bp,s} - i_f\big|_{T_i}\right) - Q_s}{\dot{m}_i\, i_{fg}\big|_{T_{h,in}}} \tag{3}$$

where $i_{bp,s}$ represent the specific enthalpy of the superheated single-phase gas derived from the temperature (T_s) and pressure (P_s) at the back-end of the bypass. These state quantities were obtained using NIST REFPROP 10 [23].

2.4. Evaluation parameters

The mass flow rate of each phase in each branch tube (vapor and liquid, $\dot{m}_{v,i}$ and $\dot{m}_{l,i}$) can be determined based on the measured individual vapor quality (x_i) using the measured individual mass flow rate ($\dot{m}_i$) of each branch tube. Similarly, from the inlet mass flow rate of the header ($\dot{m}$) and the inlet vapor quality ($x_{h,in}$), the inlet mass flow rate of the header for each phase (vapor and liquid, $\dot{m}_v$ and $\dot{m}_l$) can be derived. The flow ratio ($FR_{j,i}$) is defined as the ratio of the mass flow rate of each branch tube ($\dot{m}_{j,i}$) to the average mass flow rate of all branch tubes ($\overline{\dot{m}_j}$), for each of the vapor and liquid phases, as shown in Equation (4). From the flow ratio, the quantified nonuniformity of each branch tube can be determined.

$$FR_{j,i} = \frac{\dot{m}_{j,i}}{\overline{\dot{m}_j}} \tag{4}$$

The relative standard deviation (RSD) between the mass flow rates for each phase ($\dot{m}_{v,i}$ and $\dot{m}_{l,i}$) in each branching tube was used to assess the uniformity of the distributed two-phase flow. RSD is defined as the ratio of standard deviation to the mean. A smaller standard deviation between each branch tube, indicated by an RSD closer to zero, signifies a more uniform flow distribution. The RSD

for each phase can be calculated using Equation (5).

$$RSD_j = \frac{\sqrt{\frac{1}{n}\sum_1^n (\dot{m}_{j,i} - \bar{\dot{m}}_j)}}{\bar{\dot{m}}_j} \tag{5}$$

2.5. Data reduction and evaluation parameters

A combination of inertial, viscous, and gravitational forces typically influences the flow distribution characteristics in vertical headers. In the case of a helical-structured vertical header, centrifugal forces were introduced. We focused on understanding the effects of these additional centrifugal forces, which can be described using dimensionless numbers. The dimensionless number was derived based on parameters related to the vertical header. Fig. 3 illustrates the notation used to represent the two-phase flow distribution in the header, and each tube organized by the mass flow rate is shown in Fig. 3.

We used the Dean number [24,25] to assess the influence of the centrifugal force. The Dean number is a dimensionless number employed to analyze fluid flow behavior in a curved pipe or tube. When the fluid enters a curved section, the centrifugal force causes the flow to deviate from the main flow direction. Specifically, the fluid moves from the inside of the curve (A) to the outside (B), as observed from the cross-sectional flow of the curved section. As the fluid velocity increased, the velocity decreased on the inside of the curve (A), increasing the velocity on the outside of the curve. It generated a secondary flow (flowing from the inside of the curve to the outside) that was superimposed on the primary flow (flowing along the pipe). Consequently, a secondary flow appeared (see Fig. 4(b)). This counter-rotating flow is called a Dean vortex.

The dimensionless relationship between the primary and secondary flows can be expressed in Equation (6).

$$De_{tp} = Re_{tp}\sqrt{\frac{D_h}{2R_c}} \tag{6}$$

where the Reynolds number (Re_{tp}) corresponds to the two-phase Reynolds number at the header for the primary flow and R_c represents the radius of curvature of the helix, as shown in Equation (7).

$$R_c = r\left[1 + \left(\frac{p}{2\pi r}\right)^2\right] \tag{7}$$

We discuss the physical meaning of the Dean numbers. Fluid flow in a helical-structured channel can be visualized as a three-dimensional phenomenon, where the primary flow (along the channel) is combined with a secondary flow (across the cross-section of the channel). The magnitude of secondary flow is directly proportional to the curvature ratio ($D_h/2R_c$). When the curvature ratio exceeded unity, the secondary flow reinforced the primary flow, whereas it attenuated the primary flow when the curvature ratio was

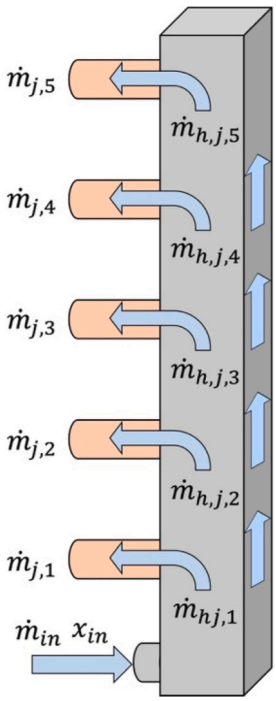

Fig. 3. Notation in the vertical header and branching tubes.

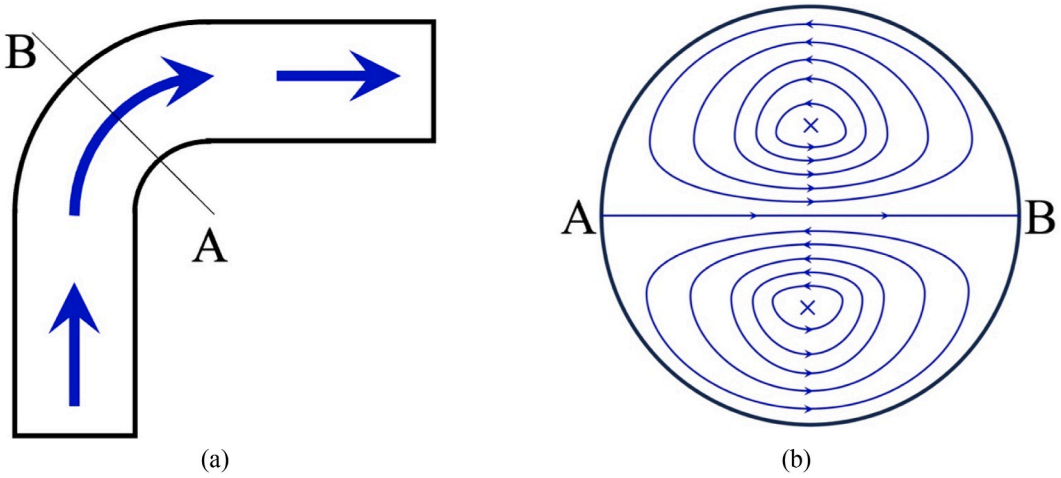

Fig. 4. Schematic of flow on the curved pipe: (a) curved flow in a pipe and (b) Dean vertex.

less than one. This signifies that the centrifugal force induced by the helical-structured functions as a compensating factor for the Reynolds number associated with the flow along the tube. As a result, the Dean number can be employed as a substitute for the Reynolds number to characterize the flow, elucidating the interplay between the inertial and viscous forces in helical coil flows.

3. Results and discussion

Fig. 5(a) and (b) depict the flow distribution profiles of the helical-structured vertical header under different experimental conditions. The profiles highlight the flow ratio and RSD for each phase, providing valuable insights into the distribution characteristics. The results obtained from our previous study [19], which involved a straight vertical header with identical height and cross-sectional geometry but lacked a helical-structured, were also included to facilitate comparison.

The results shown in Fig. 5 reveal that the helical-structured vertical header achieved a more uniform liquid distribution profile than the straight vertical header across all flow rates, except for one condition (50 kg h^{-1}, $x_{in} = 0.1$). This enhanced uniformity is corroborated by the relatively low values of the quantified distribution uniformity, as indicated by the RSD of the liquid. However, the vapor distribution profile showed that the vapor flow ratio toward the top of the header increased, except for the $x_{in} = 0.1$ condition at 50 kg h^{-1}. Moreover, the RSD of the vapor distribution was sensitive to changes in the inlet mass flow rate, exhibiting a decreasing trend as the mass flow rate increased.

To clearly understand each RSD result in Fig. 5, the liquid and vapor flow distribution profiles are analyzed in detail in the following subsections. In addition, the pressure drop of each individual channel is analyzed.

3.1. Liquid flow distribution profile

In the case of the straight vertical header, an increase in the inlet flow resulted in an increasing liquid flow ratio at the top of the header, accompanied by increasing liquid RSD (i.e., indicating poor flow distribution). Furthermore, the flow to the top of the header decreased as the inlet flow decreased and the liquid RSD decreased along with it. In contrast, the flow distribution observed in the helical-structured vertical header exhibited notable differences from that observed in the straight vertical header. On average, the liquid RSD in the helical-structured vertical header decreased by 38 % (at $x_{in} = 0.1$) to 73 % ($x_{in} = 0.2$) compared to that in the straight vertical header. Furthermore, even with the increase in inlet flow, the excessive liquid flow ratio to the top of the header, as observed in the straight vertical header for example, was not observed.

We note that the excessive increase in inertial forces has a detrimental effect on achieving a uniform flow distribution. In the author's previous work [19], we found that an excessive inlet flow rate relative to the header height leads to poor liquid flow distribution. Both helical-structured and straight vertical headers have the same cross-sectional area and height. Nevertheless, relatively uniform liquid flow rates are observed in the present study, which can be attributed to the helical structure. This can be interpreted by considering the flow characteristics in a helical flow path. In the case of the helical-structured vertical header investigated in this study, the curvature ratio ($D_h/2R_c$) is very small (0.0434), resulting in the centrifugal force induced by the helical structure damping the primary flow (Equation (6)), which can suppress the supply of excessive inertial forces.

The effect of the insufficient inertial force relative to the header height can be clearly seen in the condition of 50 kg h^{-1}. At the inlet condition of 50 kg h^{-1} and $x_{in} = 0.1$ (Fig. 5(a)), the fluid does not have enough momentum to reach the top of the header, and the liquid flow ratio in tube 5 decreases. The decrease is resolved as the inlet vapor quality increases, and at the inlet condition of 50 kg h^{-1} and $x_{in} = 0.2$, a sufficient liquid flow ratio at the top of the header can be observed. This can be attributed to the additional momentum supply due to the high velocity and large volume of the gas phase. Furthermore, a similar trend can be observed in the results for the straight vertical header, which is also indicated by the increase in the Dean number. However, the additional momentum supply due to

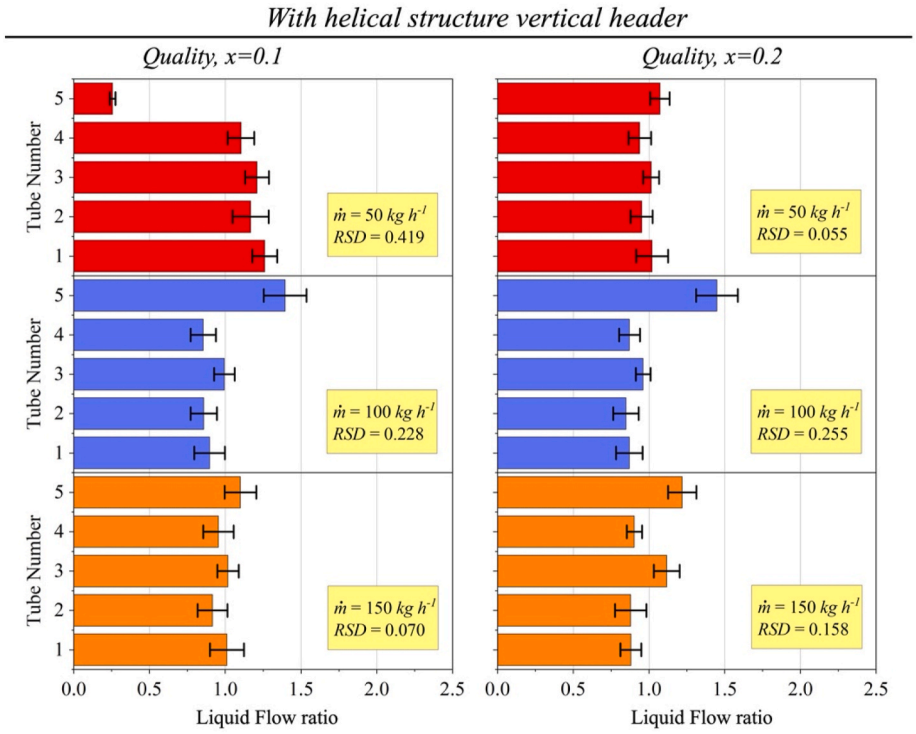

Fig. 5. Flow distribution profile of vertical header with and without helical-structured: (a) liquid distribution of helical-structured vertical header, (b) vapor distribution of helical-structured vertical header, (c) liquid distribution straight vertical header [19], and (d) vapor distribution straight vertical header [19]

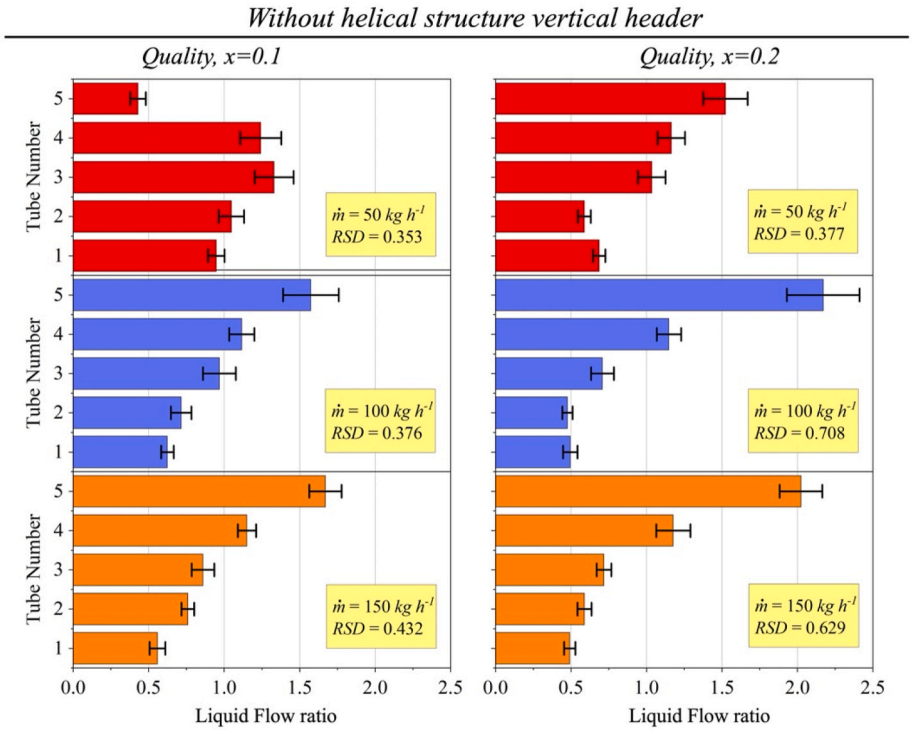

(c)

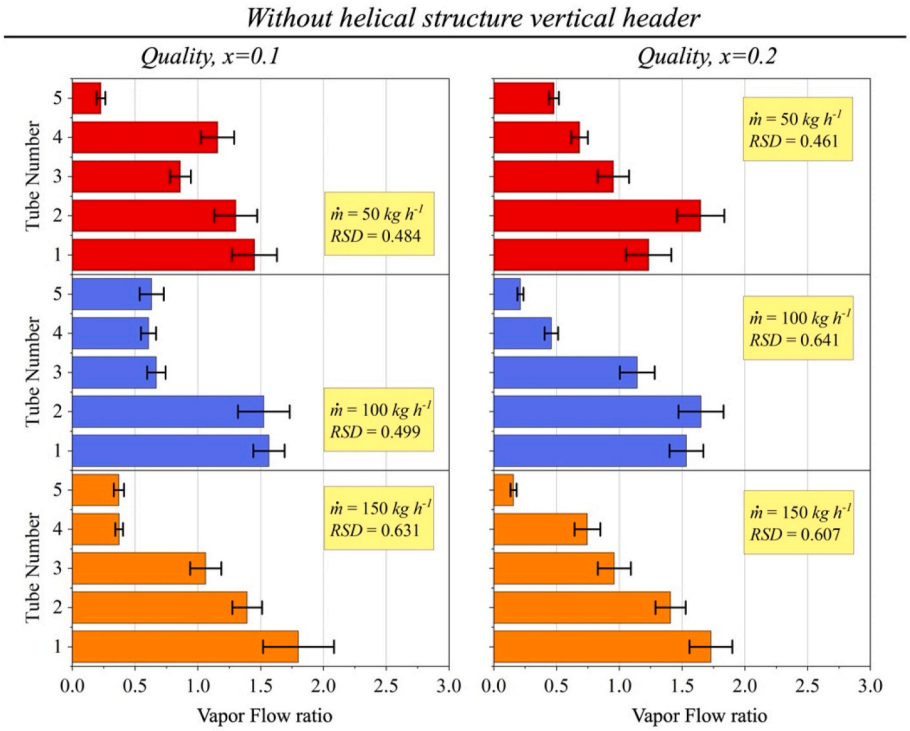

(d)

Fig. 5. (*continued*).

the increase in inlet vapor quality at different flow conditions is manifested in the excess liquid flow ratio at the top of the header, leading to an increase in the liquid RSD.

Fig. 6 compares the two-phase flow Reynolds number for the straight vertical header and the two-phase flow Dean number for the helical-structured vertical header. As described above, the Dean number in the spiral vertical header is only about 20 % (at $x_{in} = 0.1$) to 30 % (at $x_{in} = 0.2$) of the Reynold's number in the straight vertical header. As a result, the effect of inertial forces is reduced to a suitable level for the header height and allows for a relatively well distributed flow compared to a straight vertical header.

3.2. Vapor flow distribution profile

The characteristics exhibited by the helical structure were not only limited to liquid flow. However, they were also observed in vapor flow. In a typical two-phase flow, each phase flows separately and the transfer of momentum is less active. The characteristic of two-phase flow in general is well represented in the results for the straight vertical header shown in Fig. 5(c) and (d). The liquid and vapor flow distribution profiles show opposite trends; the liquid is concentrated toward the top of the header and the gas toward the bottom. However, the vapor flow distribution profile of the helical-structured vertical header was similar to the liquid flow distribution profile. Although a large deviation was observed between individual channels compared to the liquid flow, the channels with higher liquid flow ratios also increased the vapor flow ratios. The similarity between the liquid and vapor flow ratios can be attributed to the helical mixing effect [21] induced by the helical structure, facilitating a relatively well-mixed state for the gas and liquid phases.

Furthermore, a distinct characteristic was observed in the vapor flow distribution, specifically a sharp decrease in certain branch tubes (tubes 2 and 4). This phenomenon is considered inherent to the flow through a helical structure. As discussed in the numerical study conducted by Mansour et al. [21], when two dissimilar fluids undergo helical mixing, the position of each fluid reverses depending on the angle of rotation, and eventually, the fluids mix uniformly. The observations in this study can also be understood as a result of the two-phase fluid flowing along a channel with a helical structure, reversing the position of each phase and redistributing the flow into the branching tube during the process. However, a comprehensive investigation is necessary to fully understand and elucidate the mechanisms underlying this phenomenon.

As a result, the vapor RSD in the helical-structured vertical header is worse than that in the straight vertical header. For the same conditions, the increase ranges are from 4 % ($x_{in} = 0.1$) to 60 % ($x_{in} = 0.2$). The non-uniformity of the vapor flow distribution increases with the increase in inlet vapor quality, which is due to the increased momentum from the gas phase. However, it should be noted that we are more interested in the flow of the liquid phase in the distribution of the two-phase flow. This is because even if the vapor flow distribution is relatively non-uniform, if we can achieve a more uniform liquid flow distribution, it could help prevent the MCHX from failure or performance degradation.

3.3. Averaged pressure drop

In contrast, if the heat exchanger is acting as a condenser, the pressure drop would be of interest. Furthermore, the pressure drop at

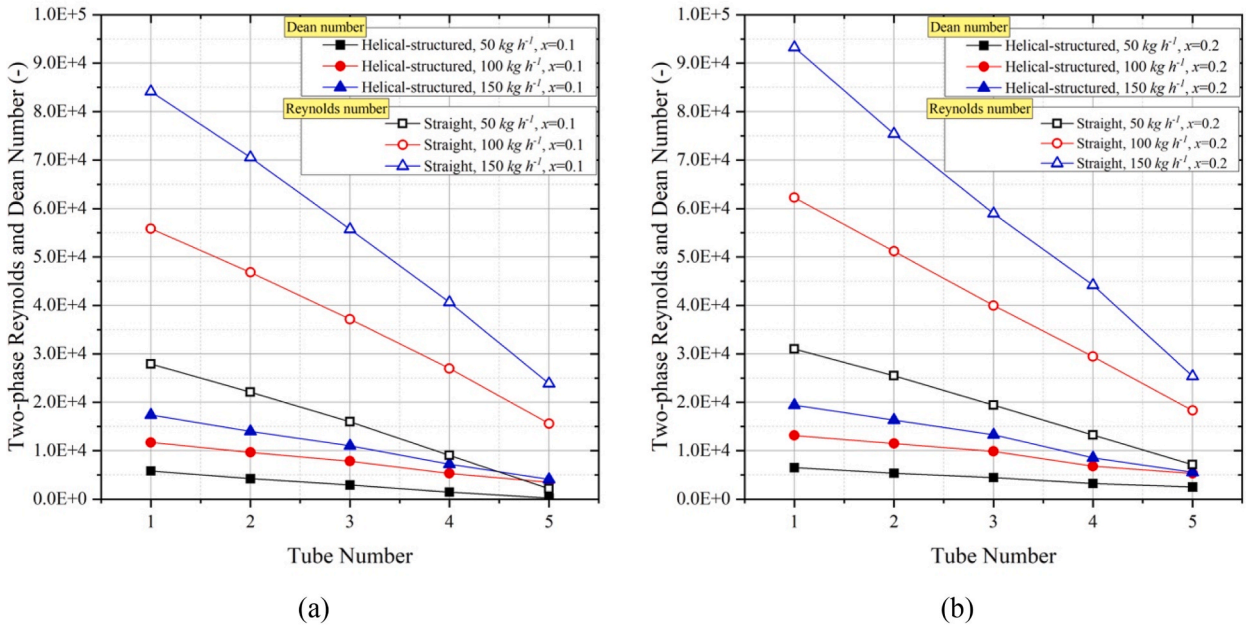

Fig. 6. Comparison of dimensionless numbers between straight and helical-structured vertical header: (a) inlet vapor quality (0.1) and (b) inlet vapor quality (0.2).

the heat exchanger header can be considered as a factor influencing the flow distribution. While pressure drop cannot fully explain the flow distribution, it can provide insight into the flow distribution. In general, at the headers with uniform flow distribution, the pressure drop will be higher. As shown in Fig. 7, the pressure drops (ΔP_i) for each individual tube were averaged and are displayed for various total inlet mass flow rates ($\dot{m}_{in}$).

The trend indicates that the averaged pressure drop increases in proportion with $\dot{m}_{in}$. Comparing the pressure drop of the helical-structured vertical header with the other two types of headers [18] at $x_{in} = 0.1$, it is approximately 40–202 % and 15–142 % greater than the conventional and dual-compartment vertical headers, respectively. At $x_{in} = 0.2$, the increase in pressure drop of the helical-structured vertical header is approximately 95–223 % and 49–150 % those of the conventional and dual-compartment vertical headers, respectively.

4. Conclusions

We investigated the flow distribution characteristics of a helical-structured vertical header by varying the inlet vapor quality (0.1, 0.2) and mass flow rate (50, 100, 150 kg h^{-1}). The flow distribution characteristics were analyzed by examining the flow ratio of each phase and evaluating the uniformity of the distributed flow using the RSD. The analysis was based on the characteristics of the flow through a helical structure. The main conclusions of this study based on the measurement results for each phase are as follows.

(1). Liquid flow distribution

The addition of a helical structure in the vertical header was found to enhance the liquid flow distribution compared to the addition of a straight vertical header with the same height; the liquid RSD decreased by 38 % and 73 % at x = 0.1 and x = 0.2, respectively. The improvement can be attributed to the interplay between the primary and secondary flows in the helical coil flow. The curvature ratio ($D/2R_c$) of the helical-structured vertical header was 0.0434; therefore, the centrifugal force attenuated the effect of the inertial force on the primary flow. The addition of a centrifugal force by the helical structure contributes to improved flow distribution by minimizing non-uniformity due to excessive inertial force relative to the height of the header.

(2). Vapor flow distribution

The helical structure causes the vapor flow distribution to have the same tendency as the liquid flow distribution. The tendency indicates that the momentum exchange between the gas and liquid phases is active. However, compared to that in the straight vertical header, the vapor flow distribution in the helical-structured header is worse; liquid RSD increased by 4 % and 60 % at x = 0.1 and x = 0.2, respectively. The above characteristics can be attributed to the helical mixing effect promoted by the Dean vortex, a secondary flow that occurs within the spiral flow.

(3). Pressure drop

The helical-structured vertical header shows an increased pressure drop compared to the header in the previous study. The results

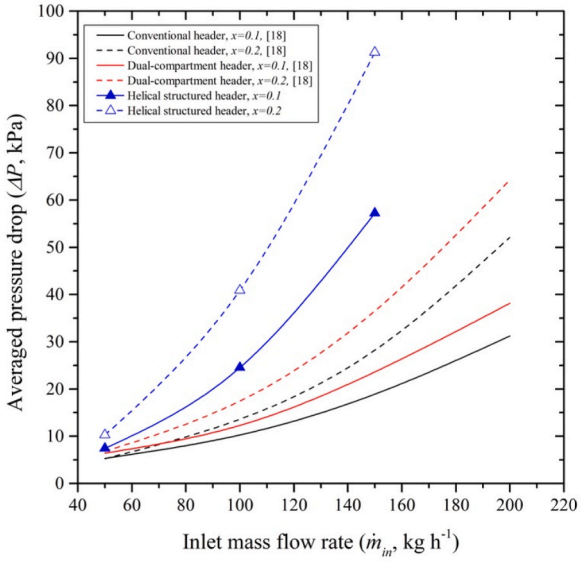

Fig. 7. Averaged pressure drop and comparison to other headers.

are attributed to an approximately 2–10 times increased mass flux due to the reduced cross-sectional area within the header. The measured pressure drop of the helical-structured vertical header is on average approximately 125 % higher than that of the other two types of vertical headers (conventional and dual-compartment).

In this study, the flow distribution characteristics were investigated by applying a spiral structure to a straight vertical header with a non-uniform two-phase distribution. Considering that the main consequences of maldistribution in heat exchangers are failures due to dry-out of some channels and performance imbalance between each channel, it is promising that a relatively uniform liquid flow distribution can be achieved by introducing a helical structure. However, the increase in structural complexity requires further physical investigation and complicates the optimization process. In future research, we expect to achieve a more comprehensive understanding of the flow inside the channel of the spiral structure through numerical analysis techniques and achieve a structurally optimal design.

Availability of data and materials

Data will be made available on request.

CRediT authorship contribution statement

Moojoong Kim: Writing – original draft, Validation, Methodology, Investigation, Formal analysis, Data curation. **Jongsoo Jeong:** Writing – review & editing, Validation, Supervision. **Kiyoshi Saito:** Writing – review & editing, Supervision, Resources, Project administration, Funding acquisition. **Sangmu Lee:** Writing – original draft, Conceptualization. **Hyunyoung Kim:** Writing – review & editing, Conceptualization.

Declaration of competing interest

The authors declare that they have no known competing financial interests or personal relationships that could have appeared to influence the work reported in this paper.

References

[1] F. Illán-Gómez, J.R. García-Cascales, F. Hidalgo-Mompeán, A. López-Belchí, Experimental assessment of the replacement of a conventional fin-and-tube condenser by a minichannel heat exchanger in an air/water chiller for residential air conditioning, Energy Build. 144 (2017) 104–116, https://doi.org/10.1016/j.enbuild.2017.03.041.
[2] B. Shen, B. Fricke, Development of high efficiency window air conditioner using propane under limited charge, Appl. Therm. Eng. 166 (2020) 114662, https://doi.org/10.1016/j.applthermaleng.2019.114662.
[3] H. Cho, K. Cho, Mass flow rate distribution and phase separation of R-22 in multi-microchannel tubes under adiabatic condition, Microscale Thermophys. Eng. 8 (2004) 129–139, https://doi.org/10.1080/10893950490445405.
[4] S. Prakash, S. Kumar, Fabrication of rectangular cross-sectional microchannels on PMMA with a CO 2 laser and underwater fabricated copper mask, Opt Laser. Technol. 94 (2017) 180–192, https://doi.org/10.1016/j.optlastec.2017.03.034.
[5] T.Q. Nguyen, W.-T. Park, Rapid, low-cost fabrication of circular microchannels by air expansion into partially cured polymer, Sensor. Actuator. B Chem. 235 (2016) 302–308, https://doi.org/10.1016/j.snb.2016.05.008.
[6] F. Botticella, F. de Rossi, A.W. Mauro, G.P. Vanoli, L. Viscito, Multi-criteria (thermodynamic, economic and environmental) analysis of possible design options for residential heating split systems working with low GWP refrigerants, Int. J. Refrig. 87 (2018) 131–153, https://doi.org/10.1016/j.ijrefrig.2017.10.030.
[7] T. Kulkarni, C.W. Bullard, K. Cho, Header design tradeoffs in microchannel evaporators, Appl. Therm. Eng. 24 (2004) 759–776, https://doi.org/10.1016/j.applthermaleng.2003.10.016.
[8] C. Amador, A. Gavriilidis, P. Angeli, Flow distribution in different microreactor scale-out geometries and the effect of manufacturing tolerances and channel blockage, Chem Eng J 101 (2004), https://doi.org/10.1016/j.cej.2003.11.031.
[9] S.G. Kandlikar, Z. Lu, W.E. Domigan, A.D. White, M.W. Benedict, Measurement of flow maldistribution in parallel channels and its application to ex-situ and in-situ experiments in PEMFC water management studies, Int. J. Heat Mass Tran. 52 (2009), https://doi.org/10.1016/j.ijheatmasstransfer.2008.09.025.
[10] E.S. Cho, J.W. Choi, J.S. Yoon, M.S. Kim, Modeling and simulation on the mass flow distribution in microchannel heat sinks with non-uniform heat flux conditions, Int. J. Heat Mass Tran. 53 (2010), https://doi.org/10.1016/j.ijheatmasstransfer.2009.12.025.
[11] A.C. Mueller, J.P. Chiou, Review of various types of flow maldistribution in heat exchangers, Heat Tran. Eng. 9 (1988) 36–50, https://doi.org/10.1080/01457638808939664.
[12] J.B. Kitto, J.M. Robertson, Effects of maldistribution of flow on heat transfer Equipment performance, Heat Tran. Eng. 10 (1989) 18–25, https://doi.org/10.1080/01457638908939688.
[13] E.R. Dario, L. Tadrist, J.C. Passos, Review on two-phase flow distribution in parallel channels with macro and micro hydraulic diameters: main results, analyses, trends, Appl. Therm. Eng. 59 (2013) 316–335, https://doi.org/10.1016/j.applthermaleng.2013.04.060.
[14] O.K. Siddiqui, S.M. Zubair, Efficient energy utilization through proper design of microchannel heat exchanger manifolds: a comprehensive review, Renew. Sustain. Energy Rev. 74 (2017) 969–1002, https://doi.org/10.1016/j.rser.2017.01.074.
[15] J.K. Lee, Two-phase flow behavior inside a header connected to multiple parallel channels, Exp. Therm. Fluid Sci. 33 (2009), https://doi.org/10.1016/j.expthermflusci.2008.03.009.
[16] Y. Hwang, D.-H. Jin, R. Radermacher, Refrigerant distribution in minichannel evaporator manifolds, HVAC R Res. 13 (2007) 543–555, https://doi.org/10.1080/10789669.2007.10390971.
[17] M.A. Redo, J. Jeong, N. Giannetti, K. Enoki, S. Yamaguchi, K. Saito, H. Kim, Characterization of two-phase flow distribution in microchannel heat exchanger header for air-conditioning system, Exp. Therm. Fluid Sci. 106 (2019), https://doi.org/10.1016/j.expthermflusci.2019.04.021.
[18] M.A. Redo, J. Jeong, S. Yamaguchi, K. Saito, H. Kim, Characterization and improvement of flow distribution in a vertical dual-compartment header of a microchannel heat exchanger, Int. J. Refrig. 116 (2020) 36–48, https://doi.org/10.1016/j.ijrefrig.2020.03.013.
[19] M. Kim, M.A. Redo, J. Jeong, K. Saito, S. Lee, H. Kim, Experimental investigation of two-phase flow distribution with different vertical header configurations, Energies 15 (2022) 8320, https://doi.org/10.3390/en15218320.
[20] P. Fei, P.S. Hrnjak, Adiabatic Developing Two-phase Refrigerant Flow in Manifolds of Heat Exchangers, 2004.
[21] M. Mansour, D. Thévenin, K. Zähringer, Numerical study of flow mixing and heat transfer in helical pipes, coiled flow inverters and a novel coiled configuration, Chem. Eng. Sci. 221 (2020) 115690, https://doi.org/10.1016/j.ces.2020.115690.

[22] M.A. Karali, M.A. Alharthi, H.A. Refaey, Influence of using different tapered longitudinal section manifolds in a Z shaped flat plate solar collector on flow distribution uniformity, Case Stud. Therm. Eng. 33 (2022) 101922, https://doi.org/10.1016/j.csite.2022.101922.
[23] E.W. Lemmon, I.H. Bell, M.L. Huber, M.O. McLinden, NIST standard reference Database 23: reference fluid thermodynamic and Transport properties-REFPROP. https://doi.org/10.18434/T4/1502528, 2018.
[24] W.R. Dean, XVI. *Note on the motion of fluid in a curved pipe*, London, Edinburgh Dublin Phil. Mag. J. Sci. 4 (1927) 208–223, https://doi.org/10.1080/14786440708564324.
[25] W.R. Dean, LXXII. *The stream-line motion of fluid in a curved pipe* (Second paper), London, Edinburgh Dublin Phil. Mag. J. Sci. 5 (1928) 673–695, https://doi.org/10.1080/14786440408564513.